CREWES www.crewes.org

Time-lapse rock physics CO_2 monitoring with FWI

Qi Hu and Kris Innanen

CREWES Sponsors Meeting
December 3, 2021

NSERC CRSNG
UNIVERSITY OF CALGARY
FACULTY OF SCIENCE
Department of Geoscience

Outline

- **Introduction**
- Methods
- Numerical examples

Introduction

- The injection of CO_2 into underground rocks for long-term storage is considered as an effective way to reduce greenhouse gas emissions.

- Time-lapse seismic data can be used to monitor the injected CO_2 and warn leakage problem if any.

- For reliable conformance verification, the monitoring should provide quantitative information on CO_2 saturation to be compared to reservoir modeling predictions.

Introduction

- **Time-lapse seismic**

Fluid saturation (t) → **Elastic properties (t)** → **Seismic response (t)**

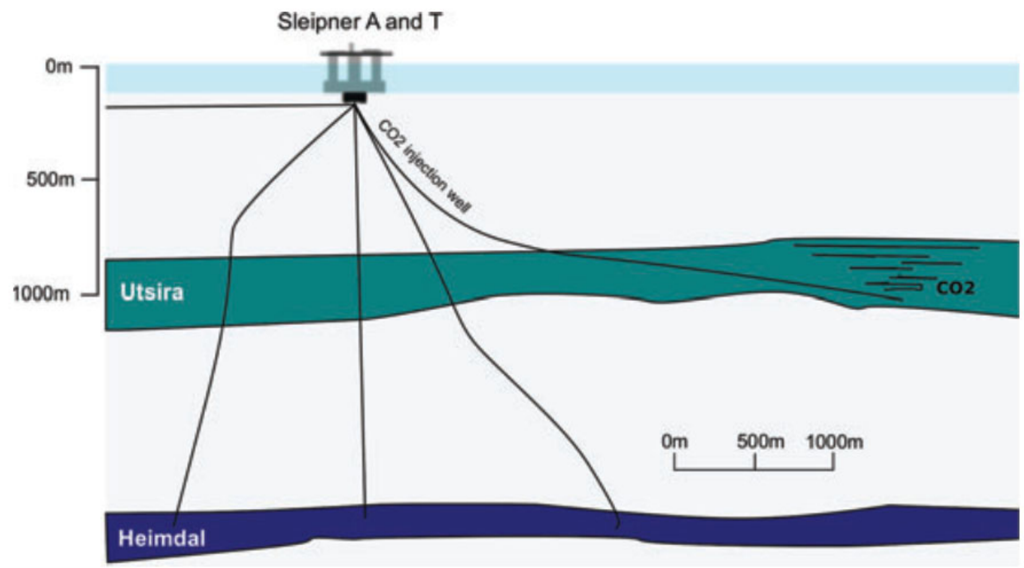

Pre-injection survey: 1994

Post-injection survey:
1999, 2001, 2002, 2004, 2006, 2008

Introduction

- **Time-lapse seismic**

Fluid saturation (t) → **Elastic properties (t)** → **Seismic response (t)**

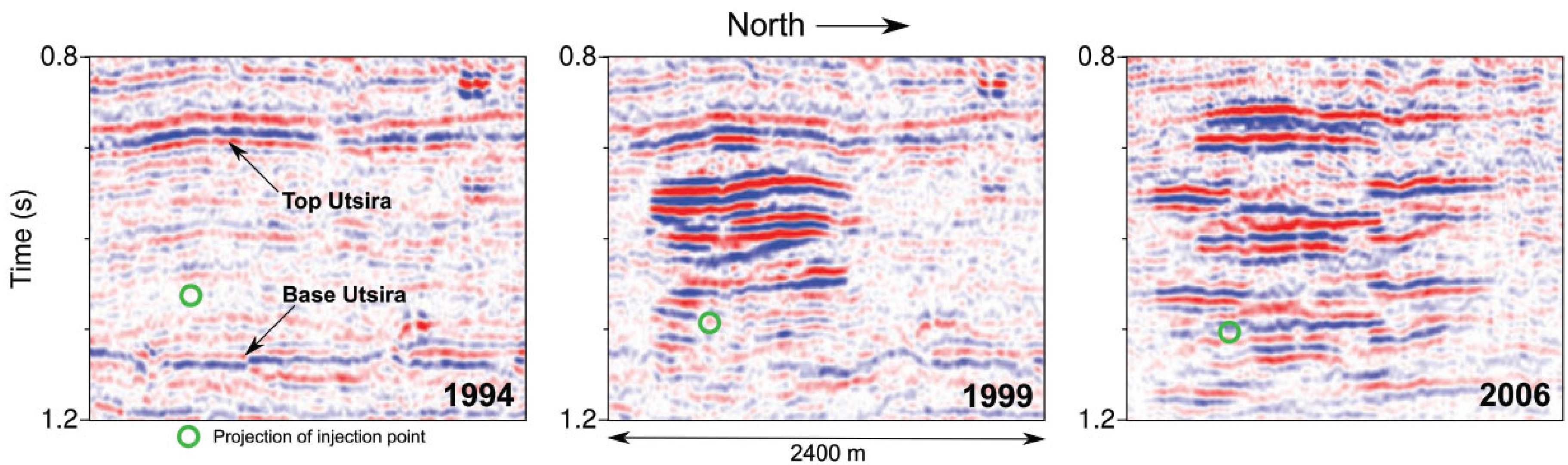

Seismic image of the growing CO2 plume at Sleipner
(Queißer and Singh, 2012)

Introduction

- **Time-lapse seismic**

Fluid saturation (t) → **Elastic properties (t)** → **Seismic response (t)**

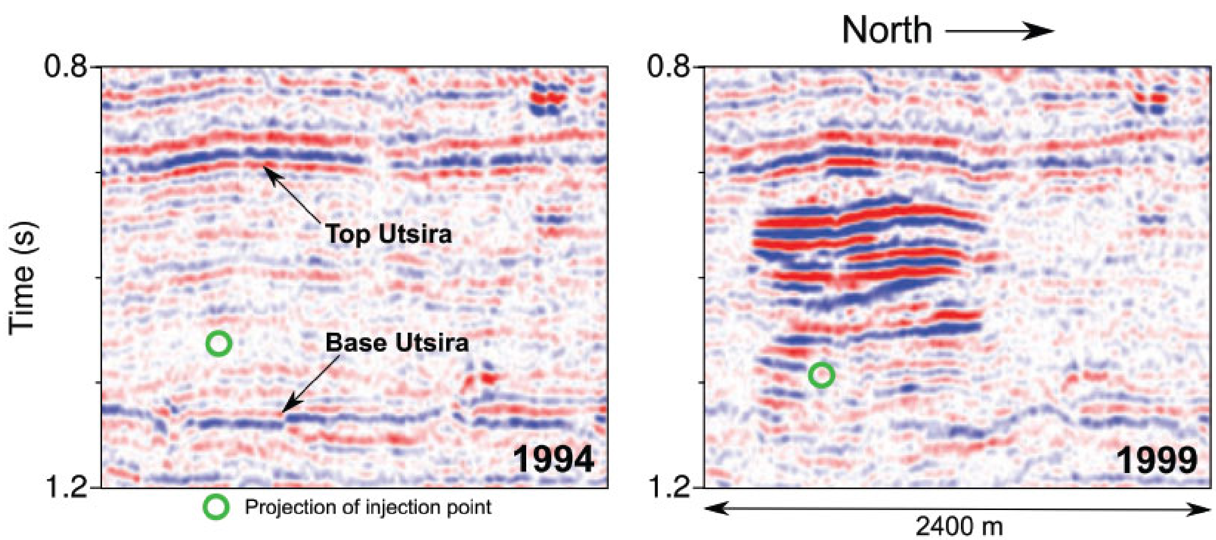

Complex wave propagation effects:

- Multiples
- Thin-layer tunning
- Attenuation
- Velocity pushdown

Introduction

- **Time-lapse seismic**

Fluid saturation (t) → **Elastic properties (t)** → **Seismic response (t)**

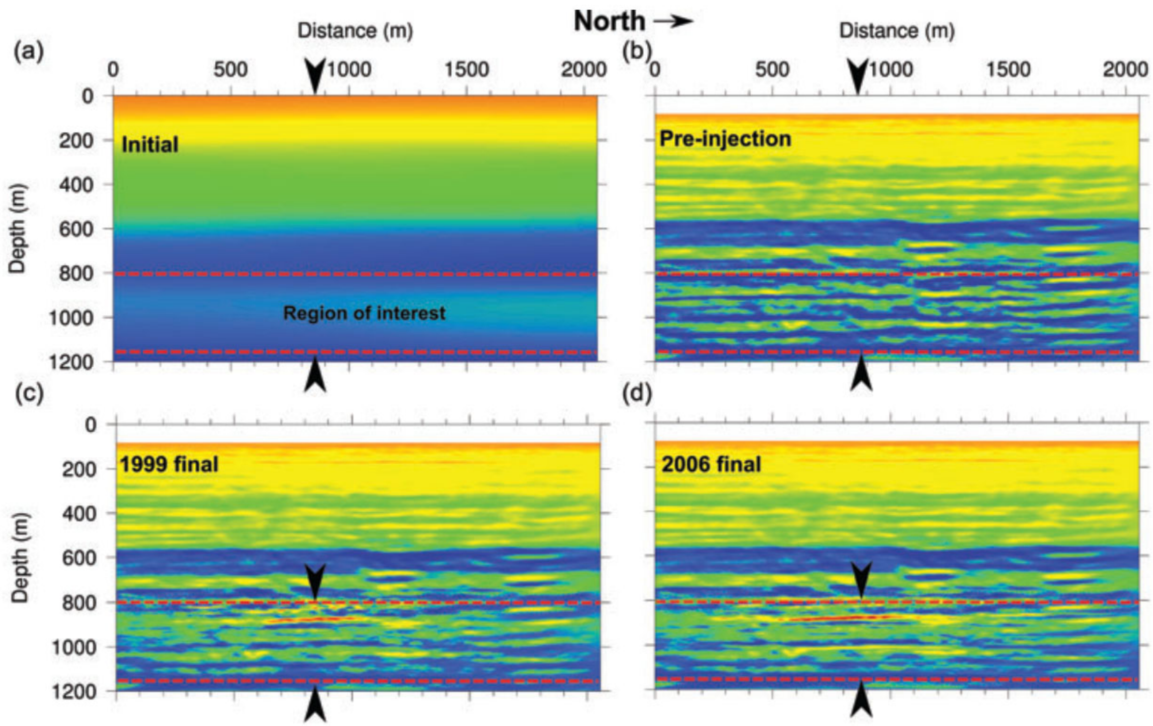

Motivations to use FWI:

- Higher resolution
- Comparison in parameter space
- Quantify time-lapse changes

Acoustic FWI result
(Queißer and Singh, 2012)

Introduction

- **Time-lapse seismic**

Fluid saturation (t) → **Elastic properties (t)** → **Seismic response (t)**

Rock physics interpretation

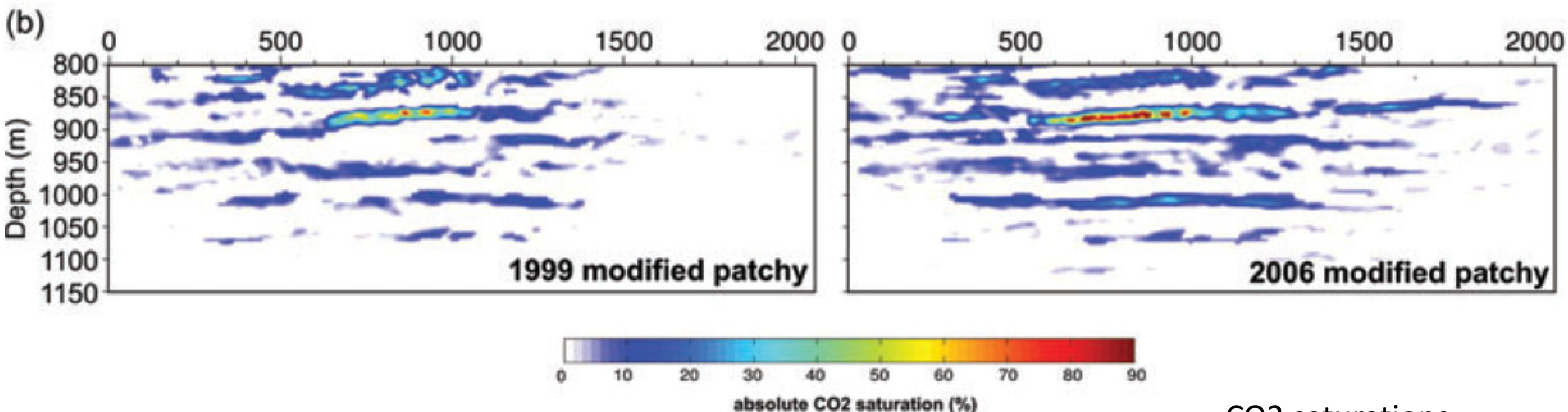

CO2 saturations
(Queißer and Singh, 2012)

Introduction

Time-lapse inversion to quantify CO_2

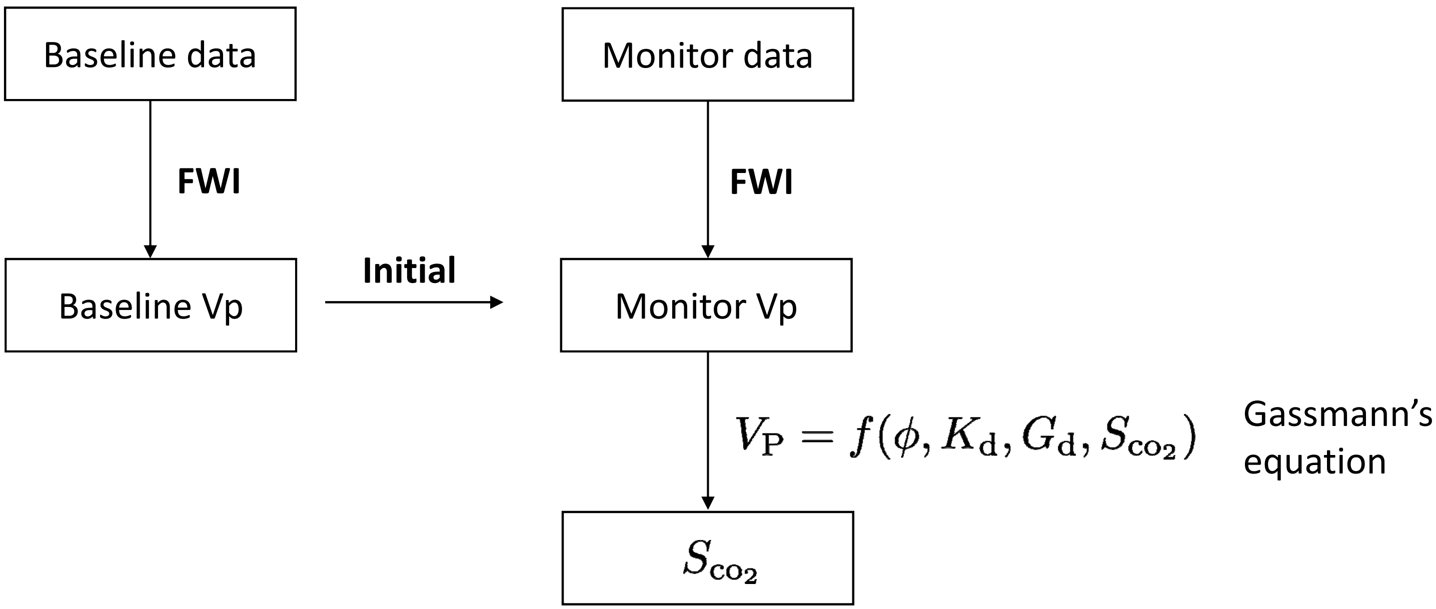

(Queißer and Singh, 2012)

Introduction

Time-lapse inversion to quantify CO_2

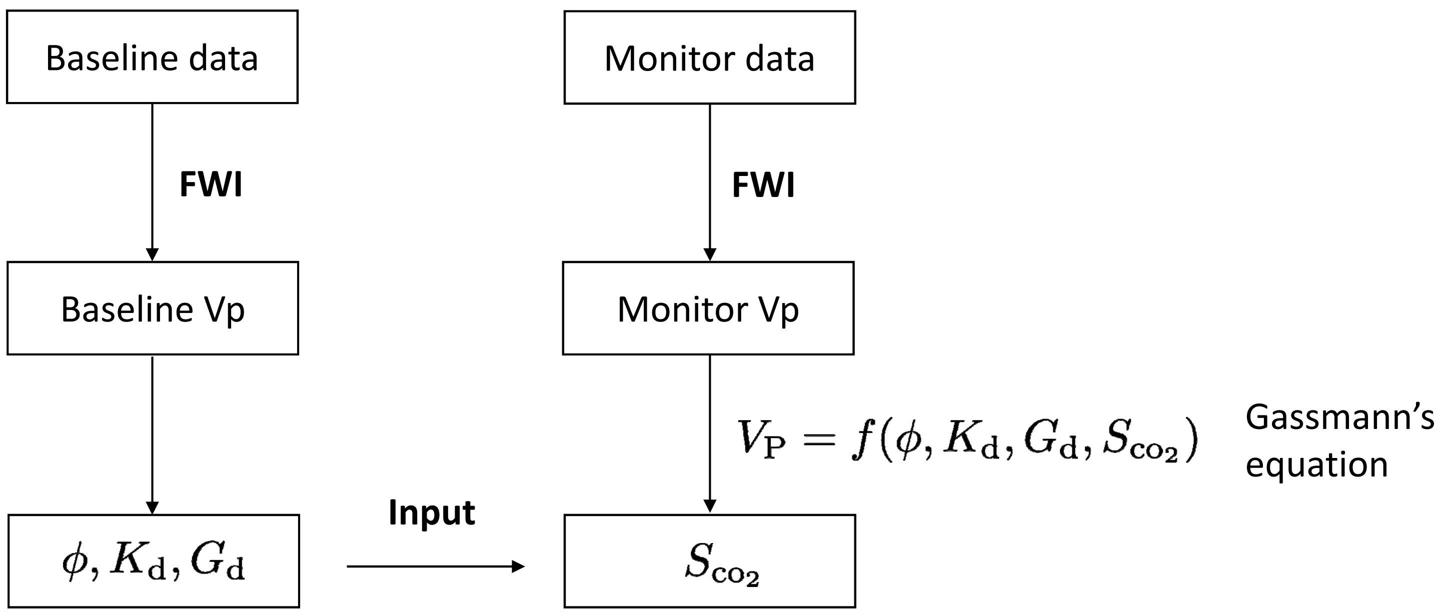

(Dupuy, 2021)

Time-lapse inversion to quantify CO_2

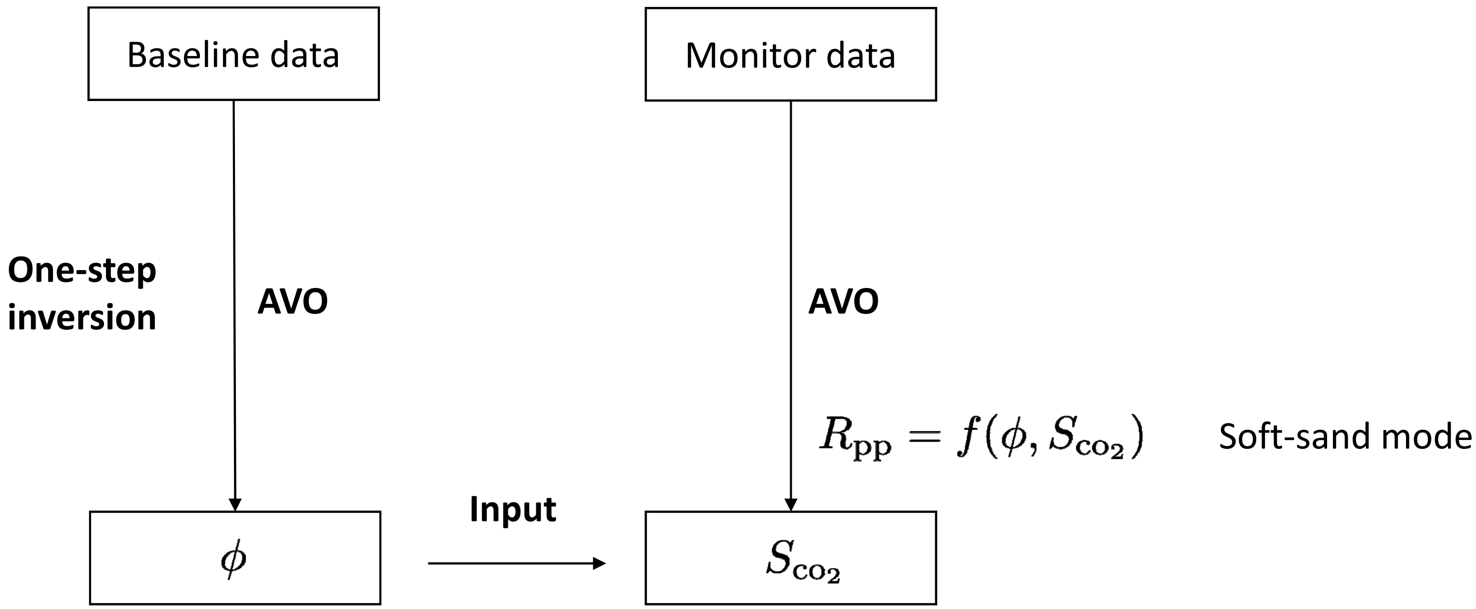

(Grana, 2020)

Introduction

Time-lapse inversion to quantify CO_2

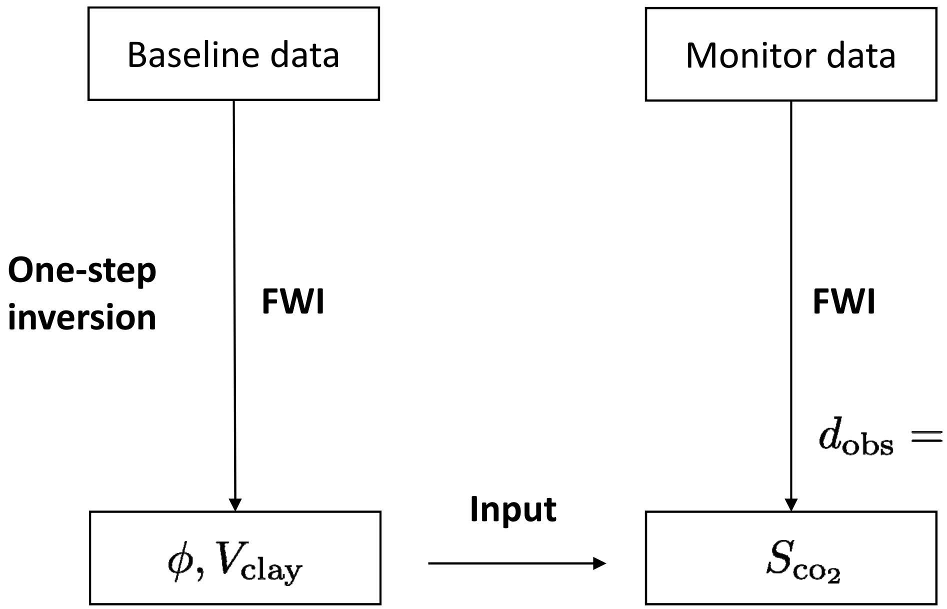

$$d_{\text{obs}} = f(\phi, V_{\text{clay}}, S_{\text{co}_2})$$

Direct rock physics FWI (Hu et al, 2021)

- Allows examination of any rock physics property that has a well-defined relationship with elastic parameters;
- Leads to a more stable solution compared to the sequential inversion;
- Shares the same numerical structure as the conventional EFWI

The proposed method

Outline

- Introduction
- **Methods**
- Numerical examples

Methods

- **Elastic FWI with rock physics parameterizations**

f: Wave propagation model

g: rock-physics model

$$\mathbf{d} = f(\mathbf{m}_e) + \mathbf{n} = f(g(\mathbf{m}_r)) + \mathbf{n}$$

$\mathbf{m}_e$: Elastic properties

(e.g., Velocity, density, modulus)

$\mathbf{m}_r$: Reservoir properties

(e.g., Porosity, Lithology, fluid saturations)

How to implement:
(2D frequency-domain)

$$\nabla_m E = \Re\left\{\mathbf{u}^t \left(\frac{\partial \mathbf{A}}{\partial m}\right)^t (\mathbf{A}^{-1})^t \Delta \mathbf{d}^*\right\}.$$

$$\frac{\partial \mathbf{A}}{\partial r_i} = \frac{\partial \mathbf{A}}{\partial e_1}\frac{\partial e_1}{\partial r_i} + \frac{\partial \mathbf{A}}{\partial e_2}\frac{\partial e_2}{\partial r_i} + \frac{\partial \mathbf{A}}{\partial e_3}\frac{\partial e_3}{\partial r_i},$$

$$(e_1, e_2, e_3) = g(r_1, r_2, ..., r_N)$$

(Hu et al, 2021)

Methods

- **Rock physics model**

Two endpoints

Solid phase ($\phi = 0$) **(Voigt-Reuss-Hill)**

Dry rock at $\phi_c \approx 0.4$ **(Hertz-Mindlin)**

Stiff-sand model:

$$K_0 = \frac{1}{2}\left[\sum_{i=1}^{N} f_i K_i + \left(\sum_{i=1}^{N} f_i/K_i\right)^{-1}\right].$$

$$K_{\mathrm{HM}} = \left[\frac{n^2(1-\phi_c)^2 G_0^2}{18\pi^2(1-v_0)^2} P_{\mathrm{e}}\right]^{1/3}$$

Interplolate $\phi \in (0, \phi_c)$ using Hashin-Strikman upper bounds

$$K_{\mathrm{dry}} = \left(\frac{\phi/\phi_c}{K_{\mathrm{HM}} + 4/3G_0} + \frac{1-\phi/\phi_c}{K_0 + 4/3G_0}\right)^{-1} - 4/3G_0,$$

Gassmann's equation:

$$K_{\mathrm{sat}} = K_{\mathrm{dry}} + \frac{(1-K_{\mathrm{dry}}/K_0)^2}{\phi/K_f + (1-\phi)/K_0 - K_{\mathrm{dry}}/K_0^2}$$

Methods

- **Rock physics FWI in the time-lapse model**

Rock type: two mineral components (quartz and clay) ; two fluid components (water and CO_2)

⇩

Model parameterization: porosity (P), clay content (C), CO_2 saturation (Sc)

Time-lapse strategies: **Baseline model reconstruction (P and C)**

Objective function:

$$E_{baseline} = \left\| \mathbf{d}_{\text{obs\_b}}(P^t, C^t, S^t_{c\_b} = 0) - \mathbf{d}_{\text{syn\_b}}(P, C, S^t_{c\_b} = 0) \right\|^2 ,$$

Monitor model reconstruction (Sc)

Objective function:

$$E_{monitor} = \left\| \mathbf{d}_{\text{obs\_m}}(P^t, C^t, S^t_{c\_m}) - \mathbf{d}_{\text{syn\_m}}(P_{\text{inv}}, C_{\text{inv}}, \boxed{S_{c\_m}}) \right\|^2 ,$$

Outline

- Introduction
- Methods
- **Numerical examples**

Numerical examples

- **The Johansen Formation Model**

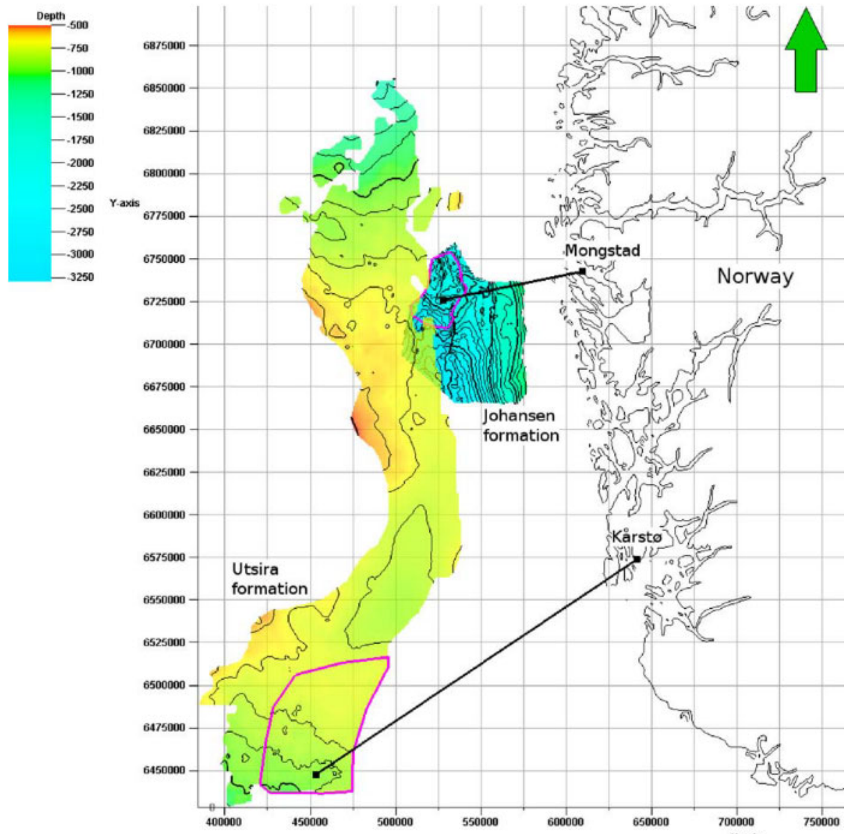

Bergmo (2010)

Porosity:

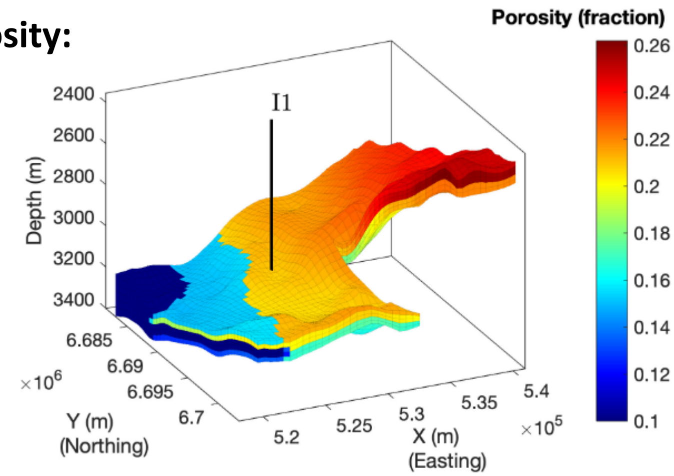

Simulated CO_2

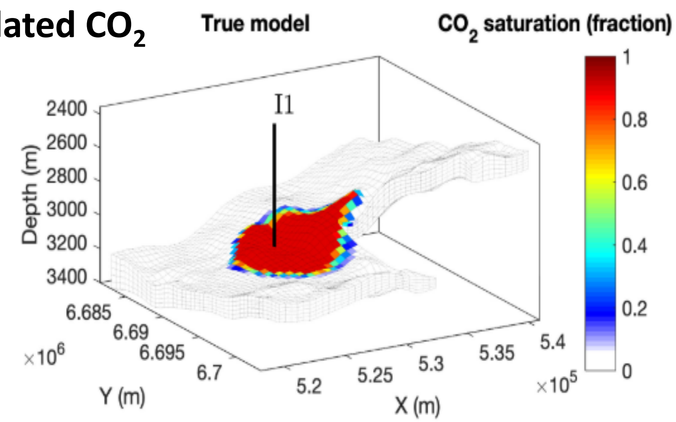

Grana (2020)

Numerical examples

- **2D version**

Original model (sparse samples)

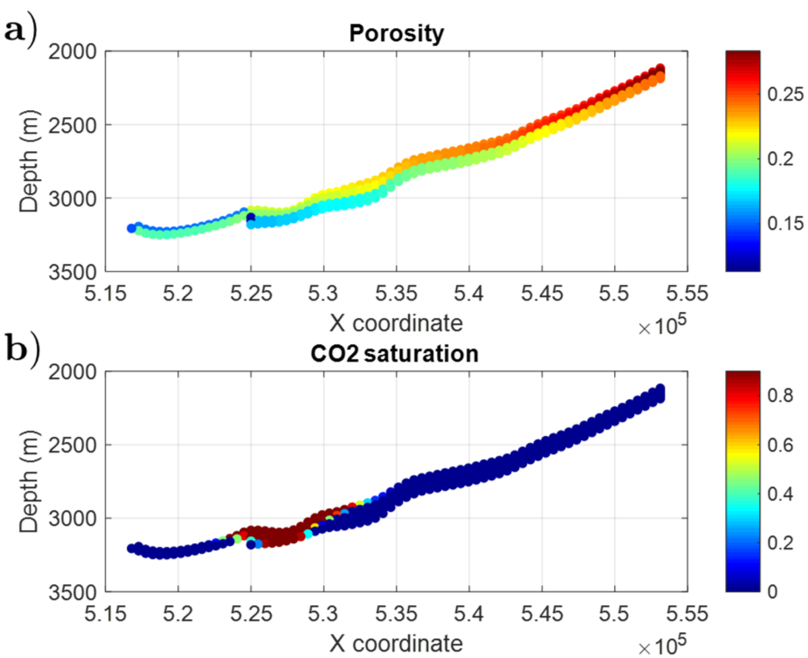

Created model (regular grid, 76×81, dx=dz=10 m)

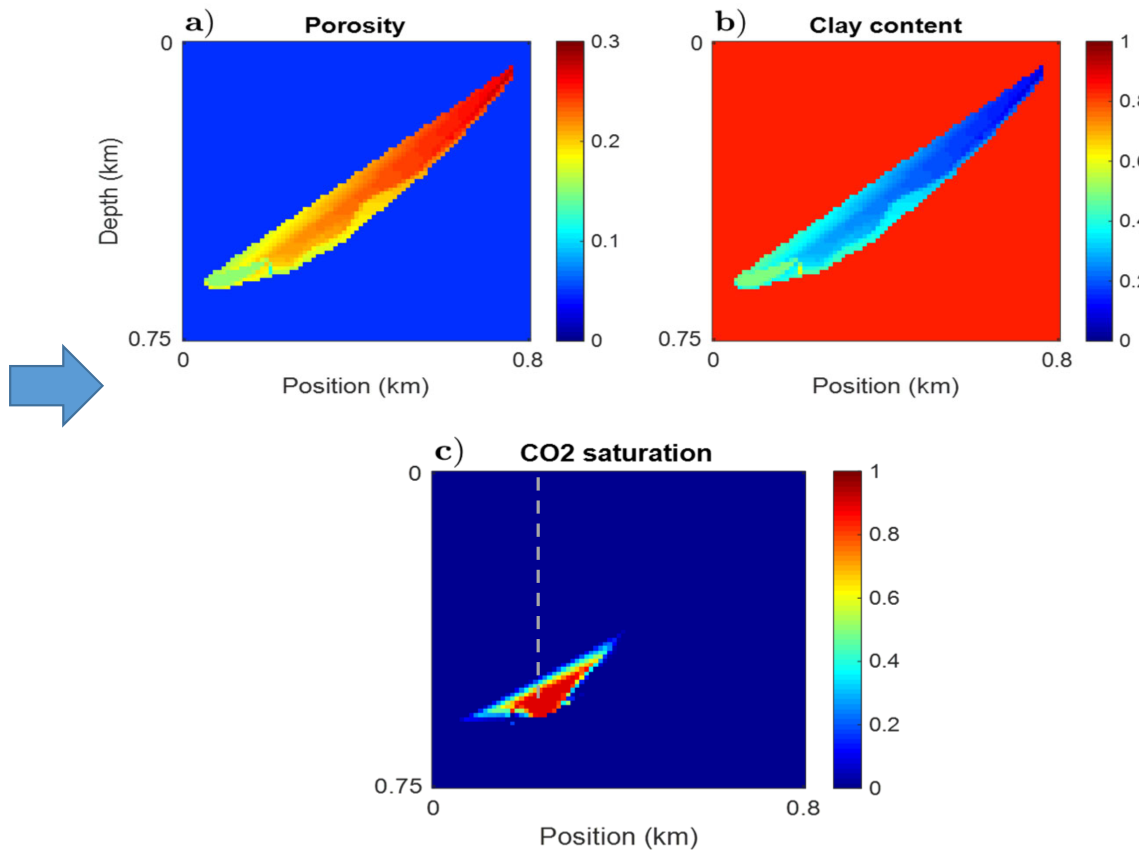

Numerical examples

- **Baseline model reconstruction**

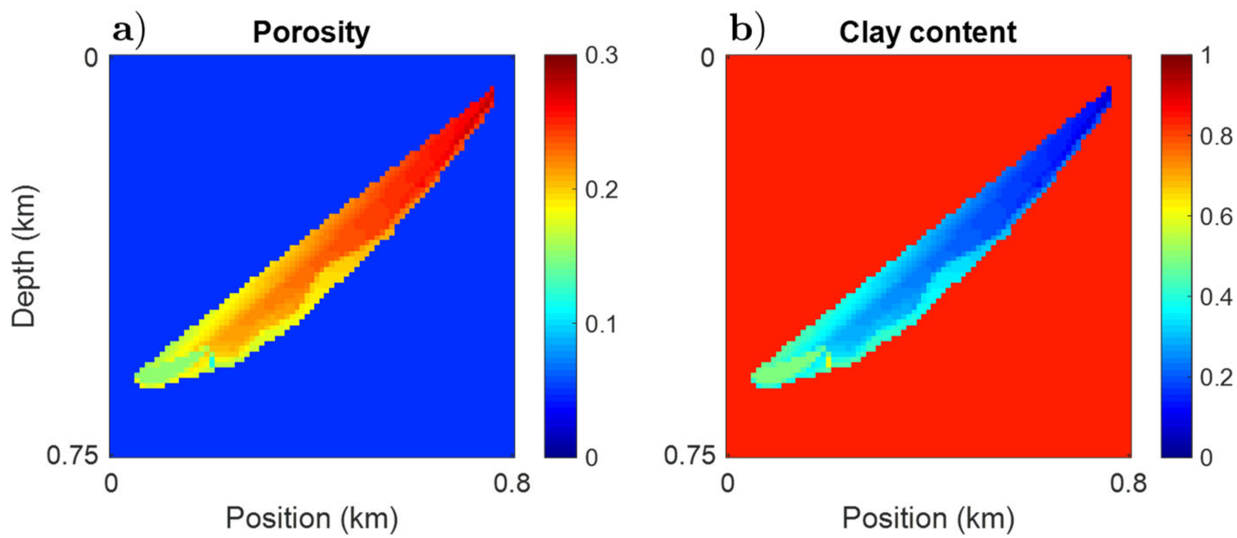

Numerical examples

- **Initial models: realistic in terms of assumptions of what we know**

1. Subsample the true model and interpolate on the original grid

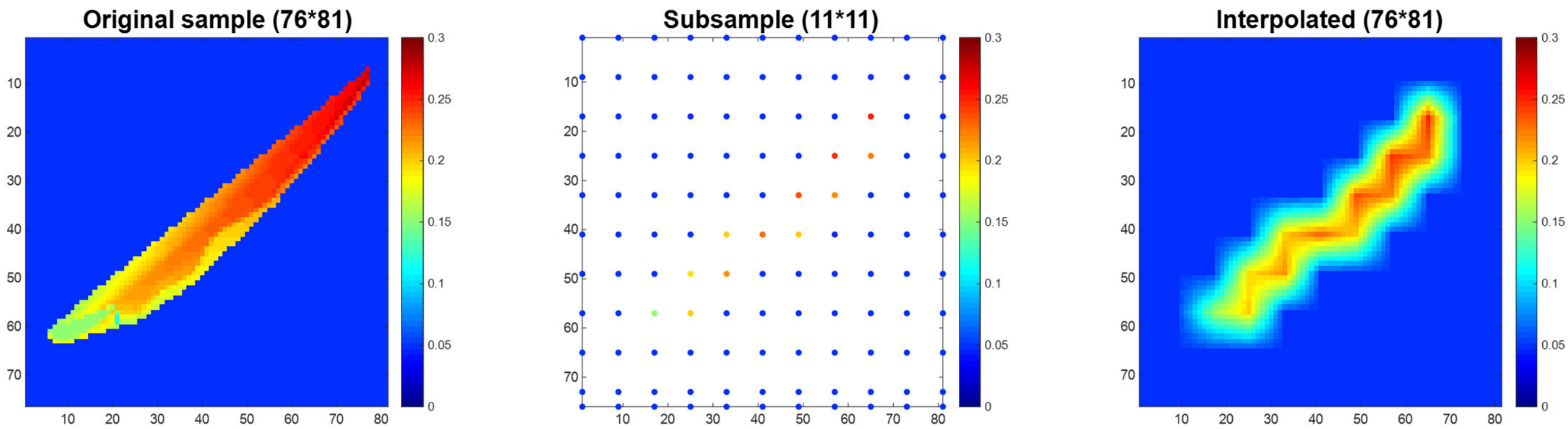

Numerical examples

- **Initial models**

2. filter the true model of velocity and apply a linear regression for porosity.

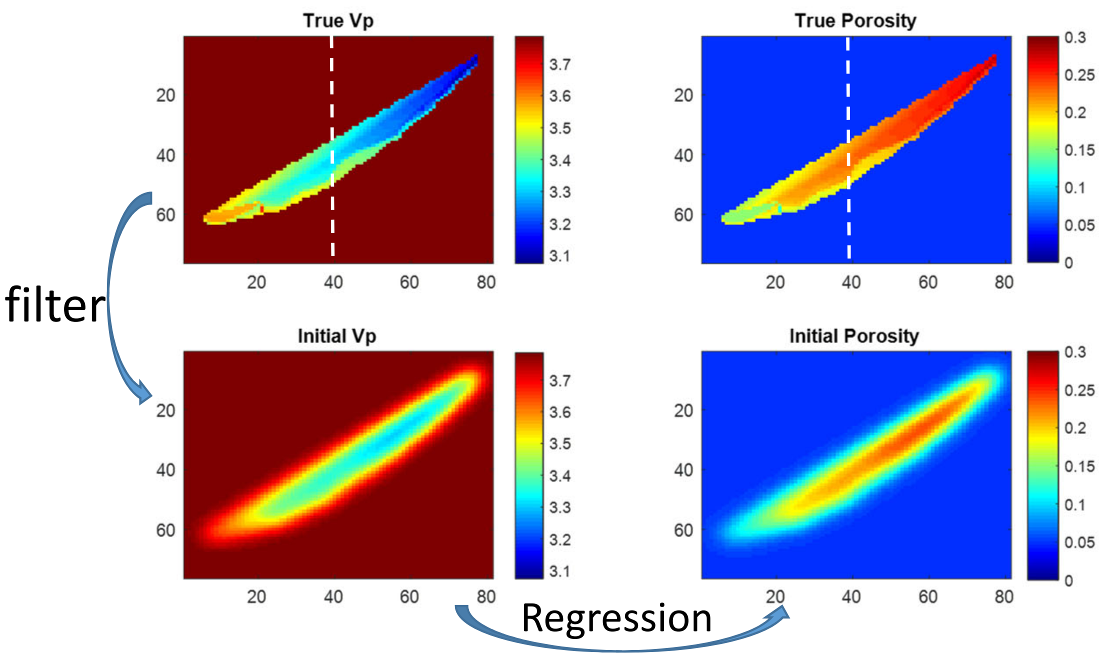

The well data at x=0.4 km are used to build a velocity-porosity relationship

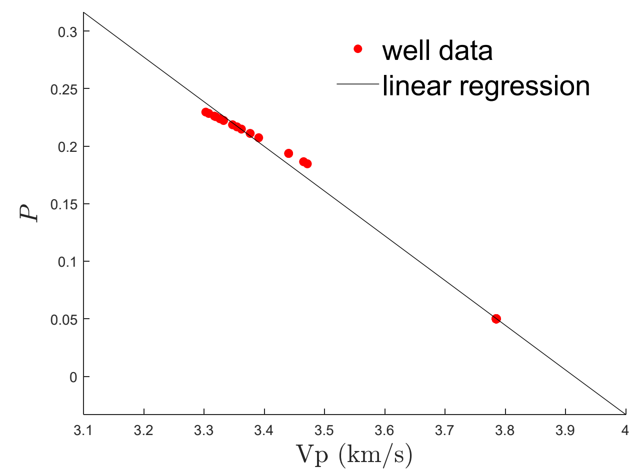

Numerical examples

- **Initial models**

3. Set constant rock physics properties in each layer (assuming the exact horizons are known).

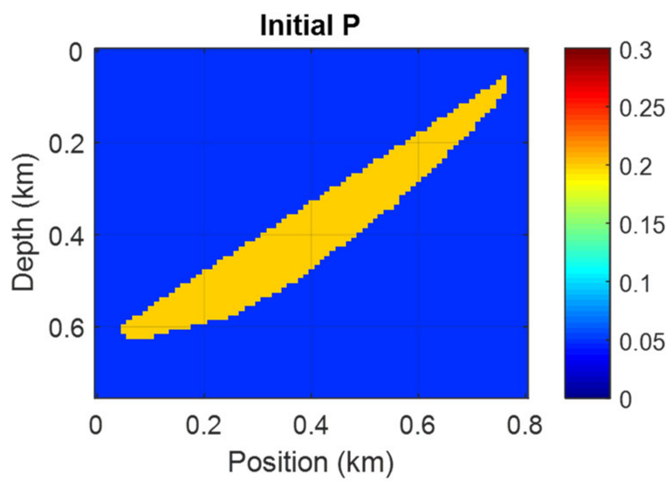

Numerical examples

- **3 initial models**

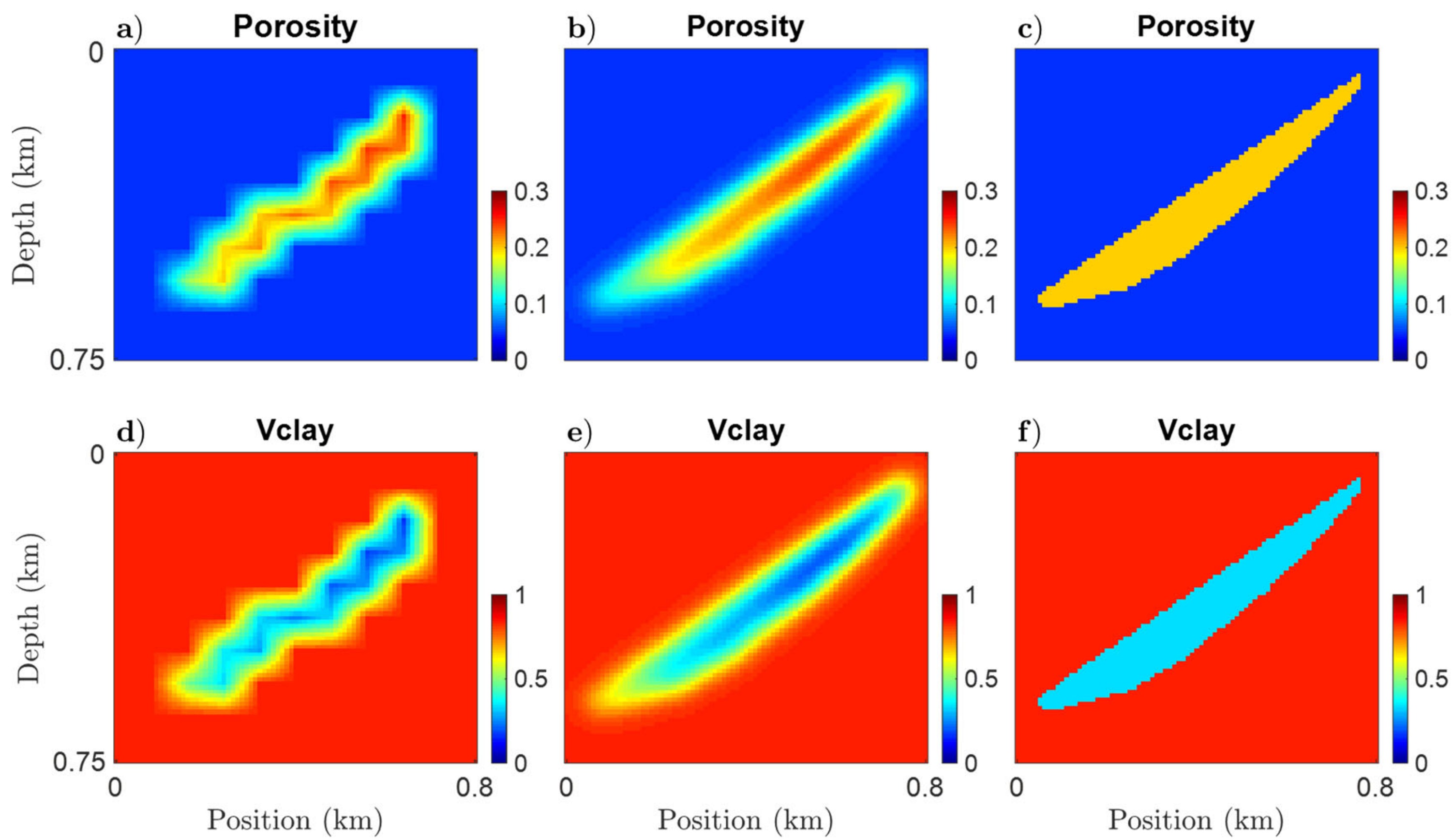

Numerical examples

- **Inverted models starting from the 3 initial models**

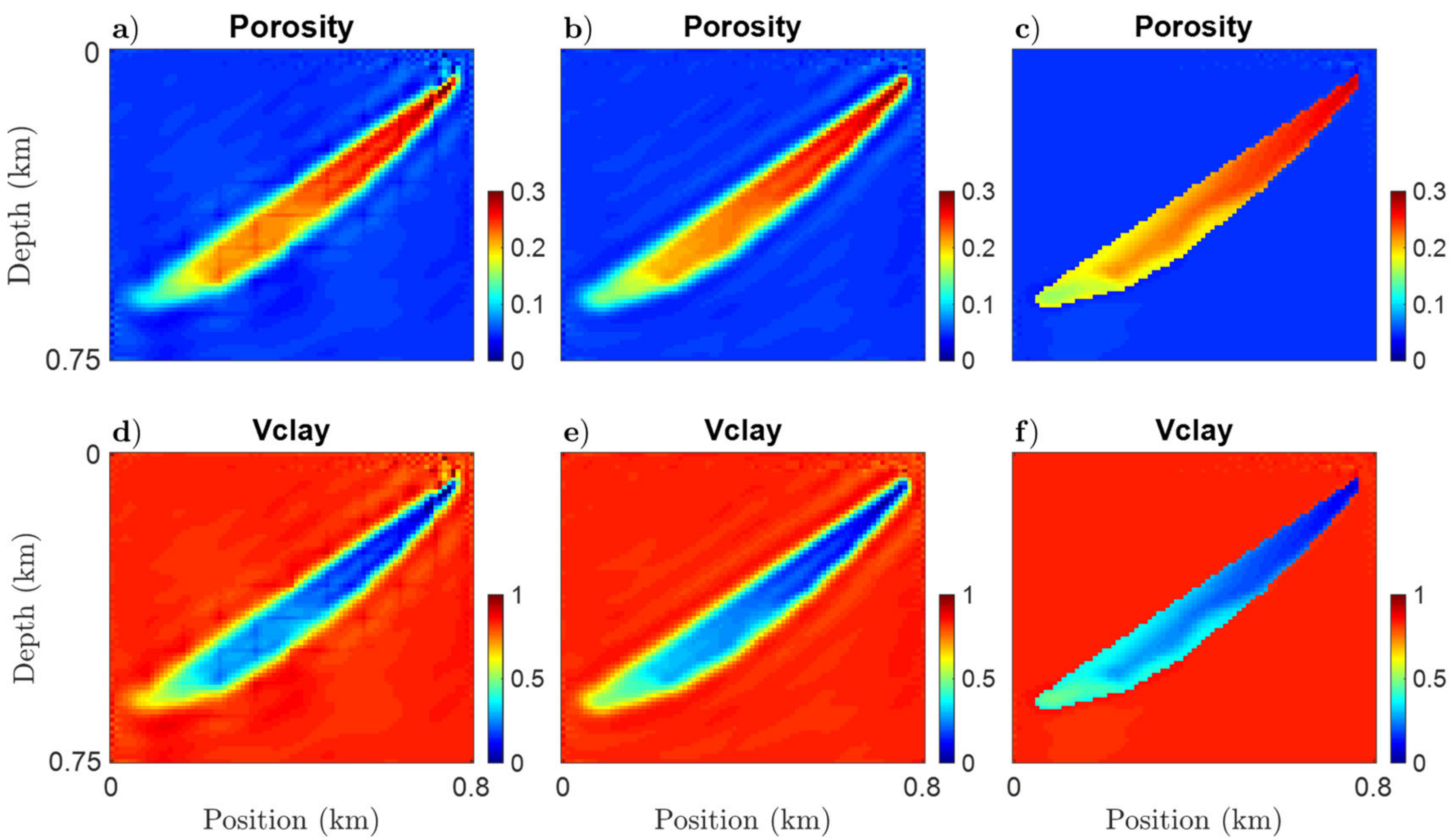

Numerical examples

- **Comparison between the inversion results**

Model profiles at x=0.4 km

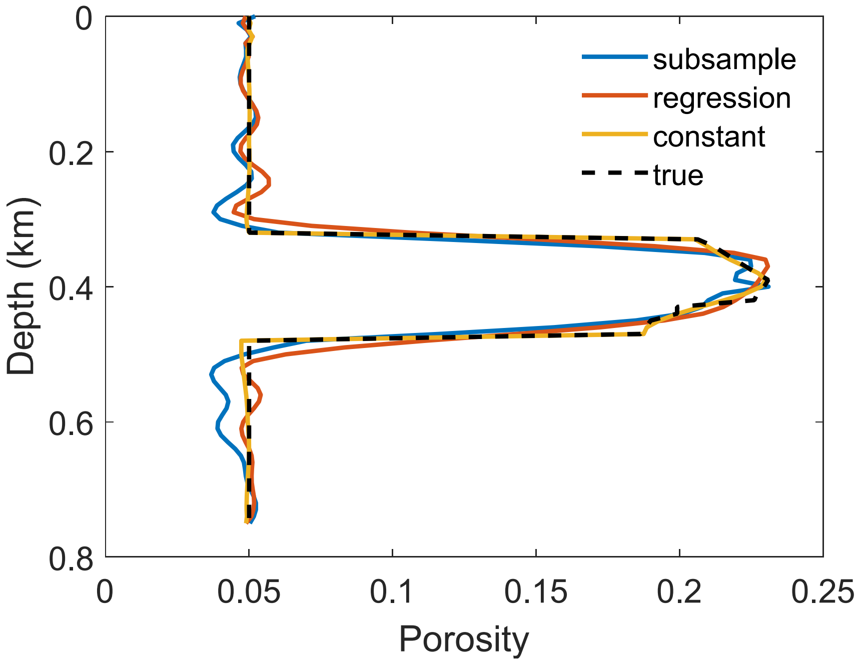

History of model error reductions

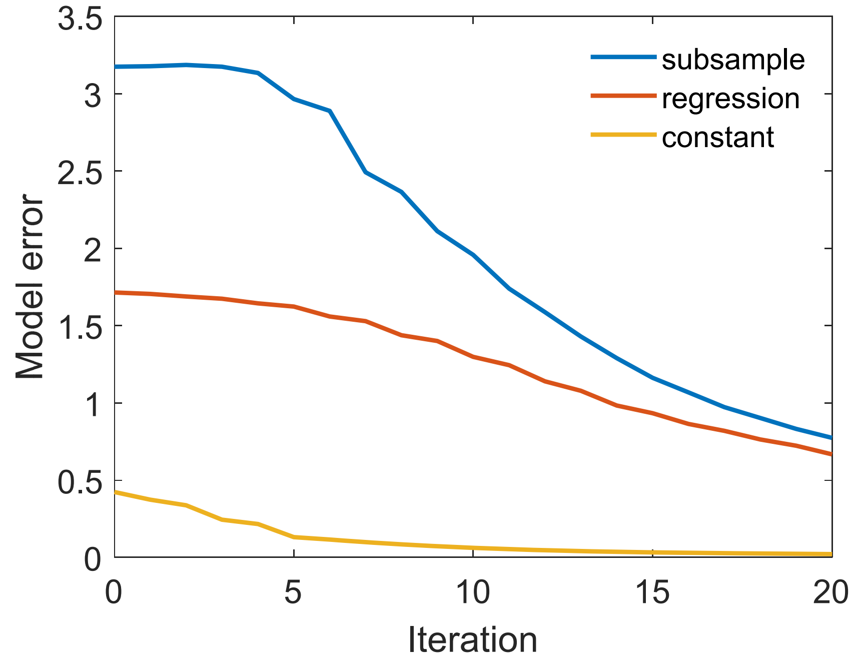

Numerical examples

- **Inverted models with noisy data (S/R=10)**

Used as input in the monitor survey

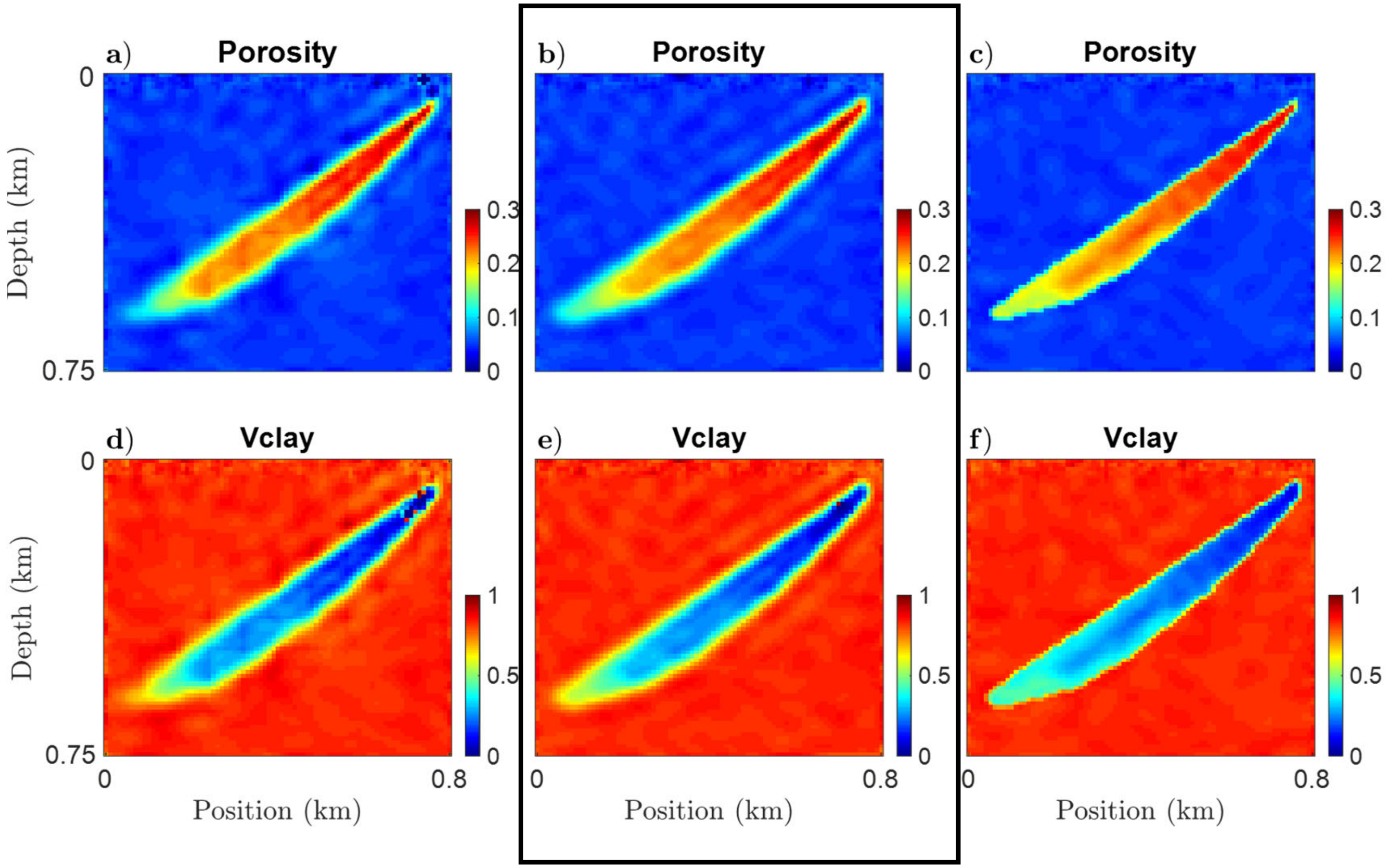

Numerical examples

- **Monitor model reconstruction**

Objective function:

$$E_{monitor} = \left\| \mathbf{d}_{\mathrm{obs\_m}}(P^t, C^t, S^t_{c\_m}) - \mathbf{d}_{\mathrm{syn\_m}}(P_{\mathrm{inv}}, C_{\mathrm{inv}}, \boxed{S_{c\_m}}) \right\|^2,$$

$$\mathbf{d}_{\mathrm{obs\_m}} = f(P^t, C^t, S^t_{c\_m}) + \underline{\mathbf{noise}}$$

$$\mathbf{d}_{\mathrm{syn\_m}} = f(\underline{P_{\mathrm{inv}}, C_{\mathrm{inv}}}, S_{c\_m})$$

Uncertainties in the estimation of CO_2

Numerical examples

- **How errors in baseline model estimates affect the estimation of CO_2**

Reference 1: Poorly estimated **Reference 2: Perfectly estimated**

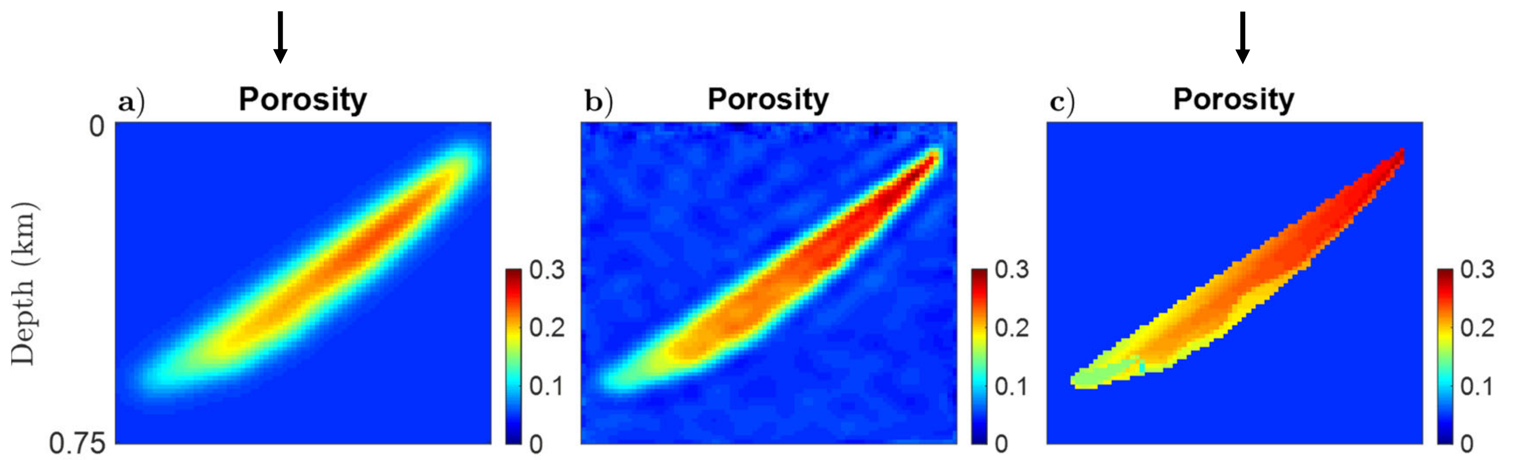

Numerical examples

- **How do errors in baseline model estimates affect the estimation of CO_2**

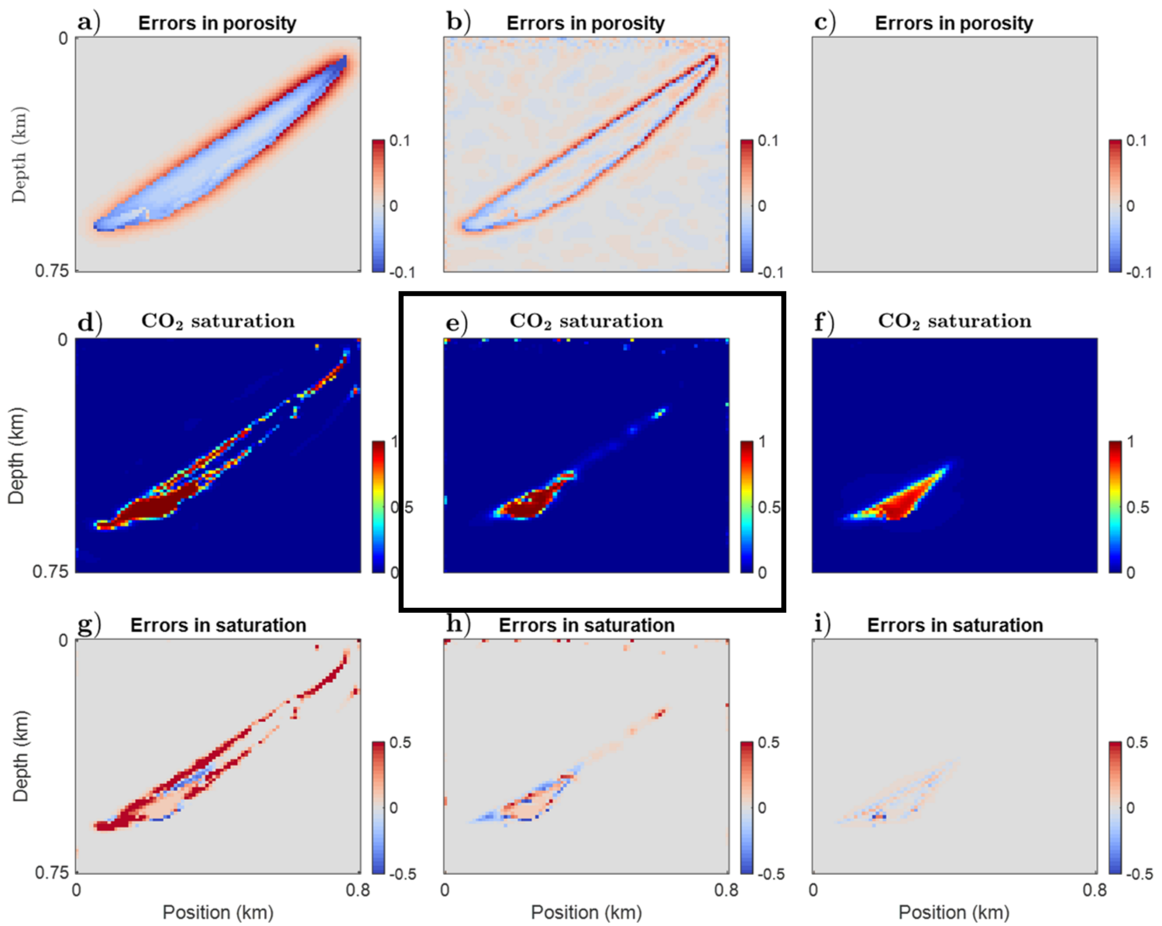

Numerical examples

- **Errors in baseline model estimates + random noise effects**

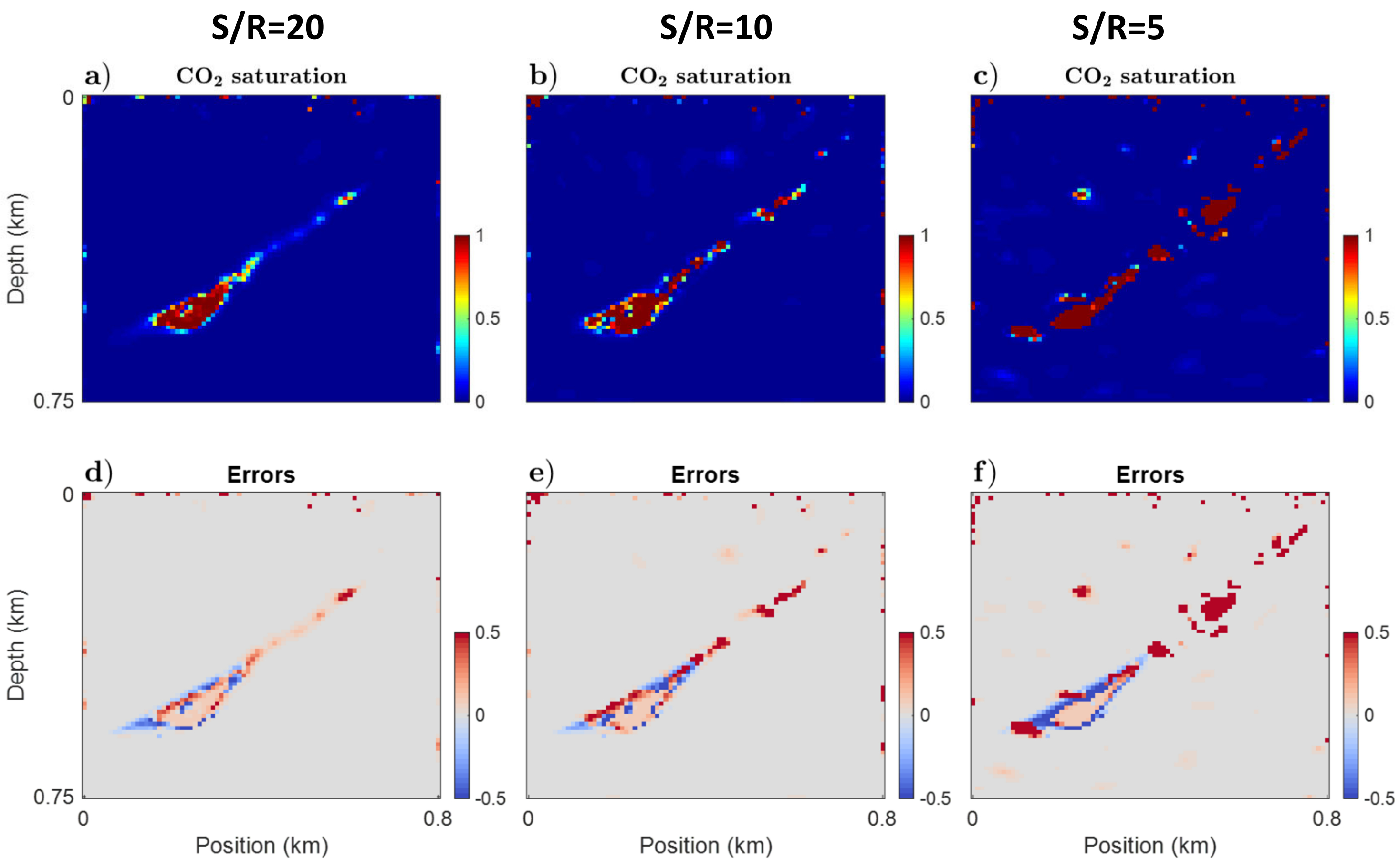

Numerical examples

$$E_{monitor} = \left\| \mathbf{d}_{\mathrm{obs\_m}}(P^t, C^t, S^t_{c\_m}) - \mathbf{d}_{\mathrm{syn\_m}}(P_{\mathrm{inv}}, C_{\mathrm{inv}}, \boxed{S_{c\_m}}) \right\|^2,$$

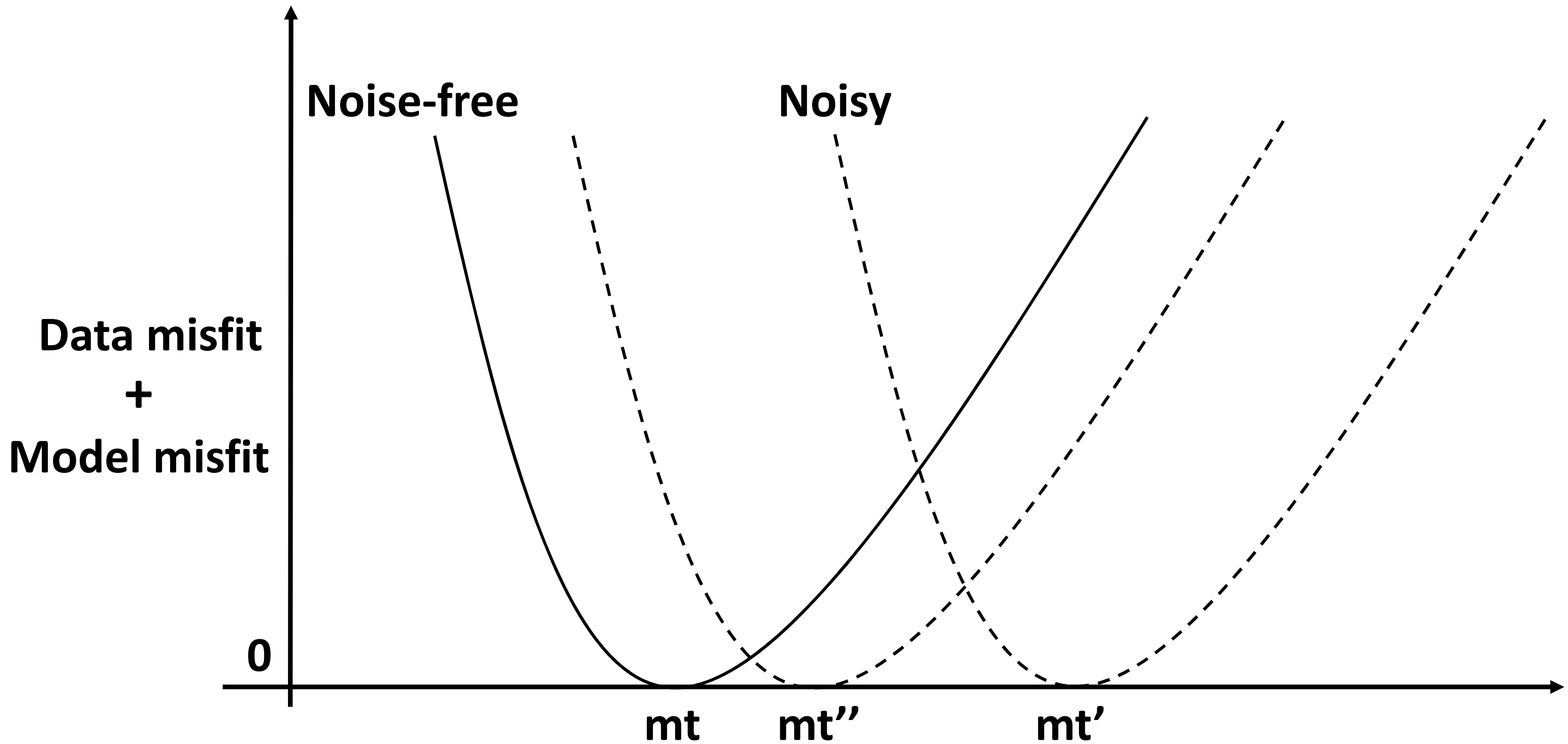

Numerical examples

Regularization

$$E = E_d + \lambda E_m$$

Objective function Data misfit Model penalty

First-order Tikhonov regularization:

$$E_m = \|\mathbf{D}_x\mathbf{m}\|^2 + \|\mathbf{D}_z\mathbf{m}\|^2$$

First-order spatial derivative operators

This regularization assumes that neighboring points in the model should be close in value, leading to smooth solutions.

Numerical examples

- **Errors in baseline model estimates + random noise effects**

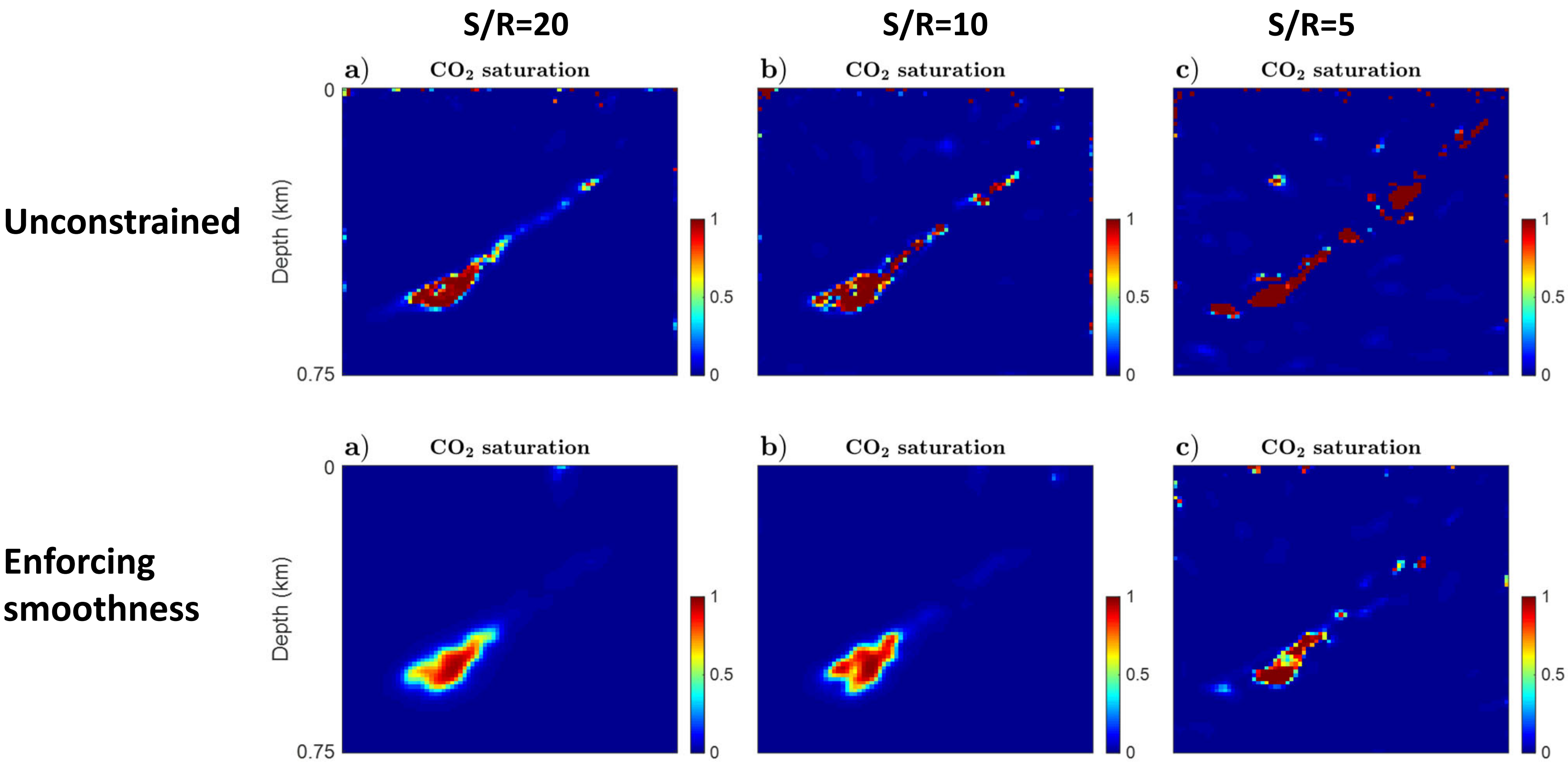

Numerical examples

Regularization

$$\underset{\text{Objective function}}{E} = \underset{\text{Data misfit}}{E_d} + \lambda \underset{\text{Model penalty}}{E_m}$$

Prior model constraint:

$$E_m = \|\underset{\text{Weighting matrix}}{\mathbf{W}_m}(\mathbf{m} - \underset{\text{Prior model}}{\mathbf{m_p}})\|^2$$

Sometimes we have a very good reference (or prior) model, and we do not want the inverted model to deviate much from the prior model

Numerical examples

Prior model constraint: $E_m = \|\mathbf{W}_m(\mathbf{m} - \mathbf{m_p})\|^2$

Prior model

True model

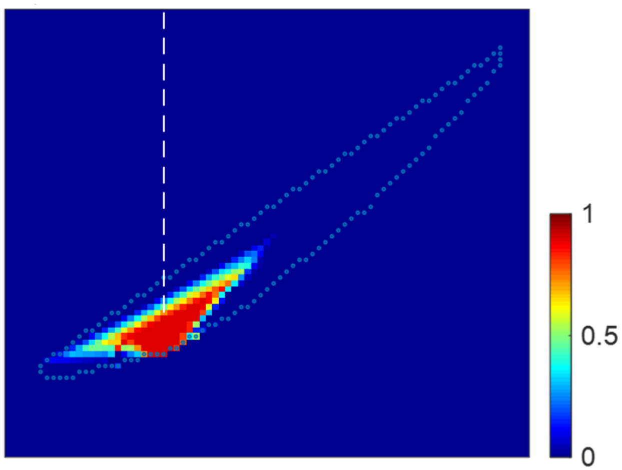

Prior model

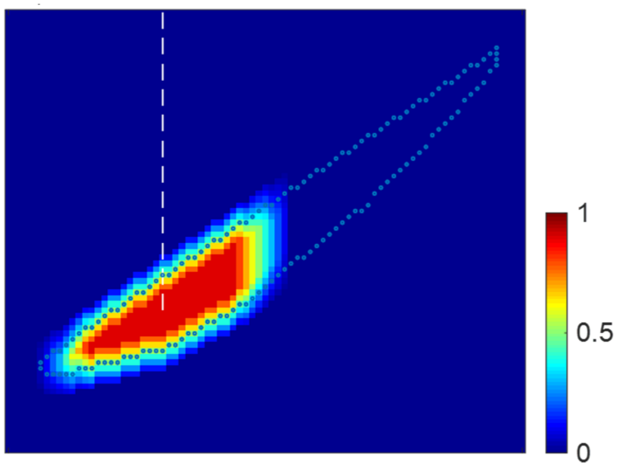

Numerical examples

- **Errors in baseline model estimates + random noise effects**

S/R=20 **S/R=10** **S/R=5**

Unconstrained

Prior model Constraint

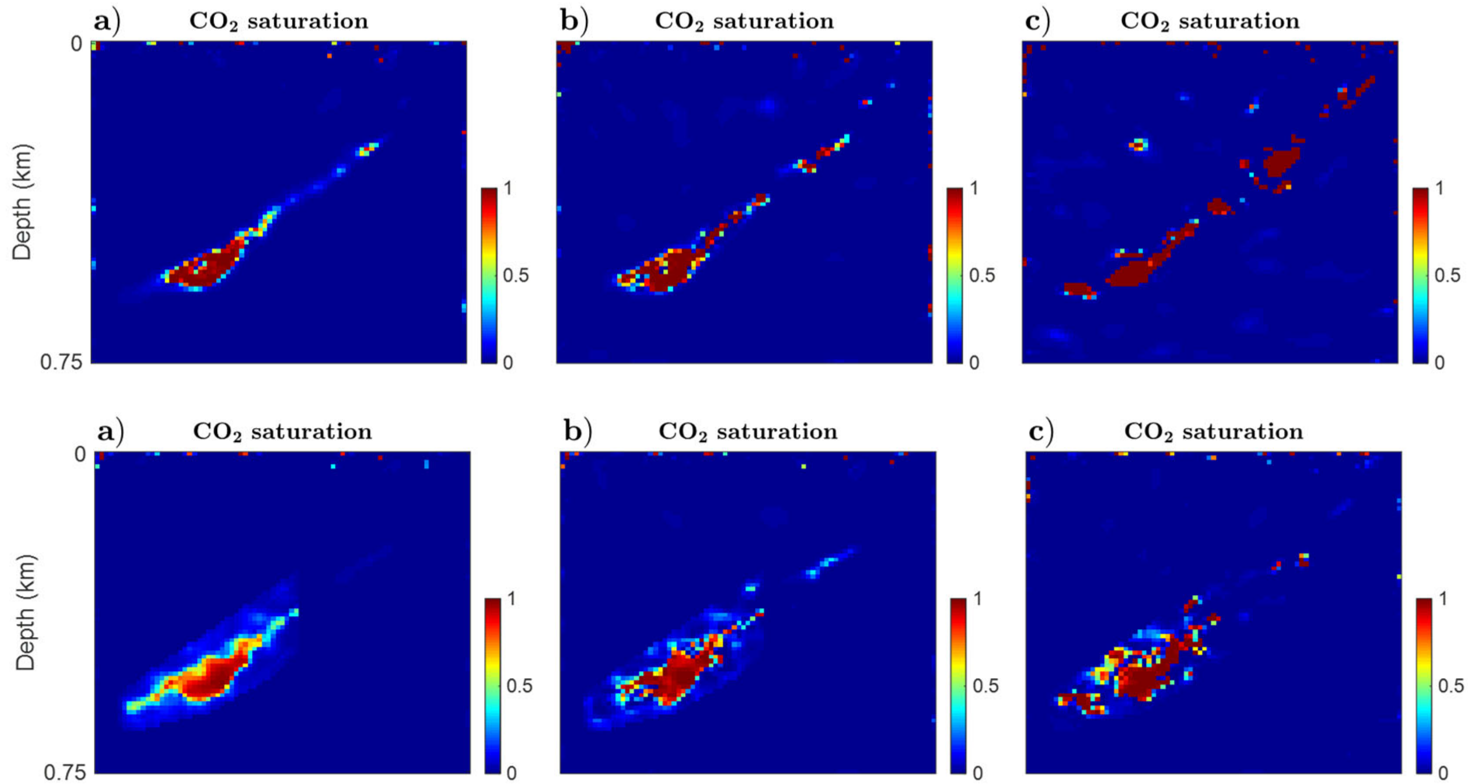

Numerical examples

- **Errors in baseline model estimates + random noise effects**

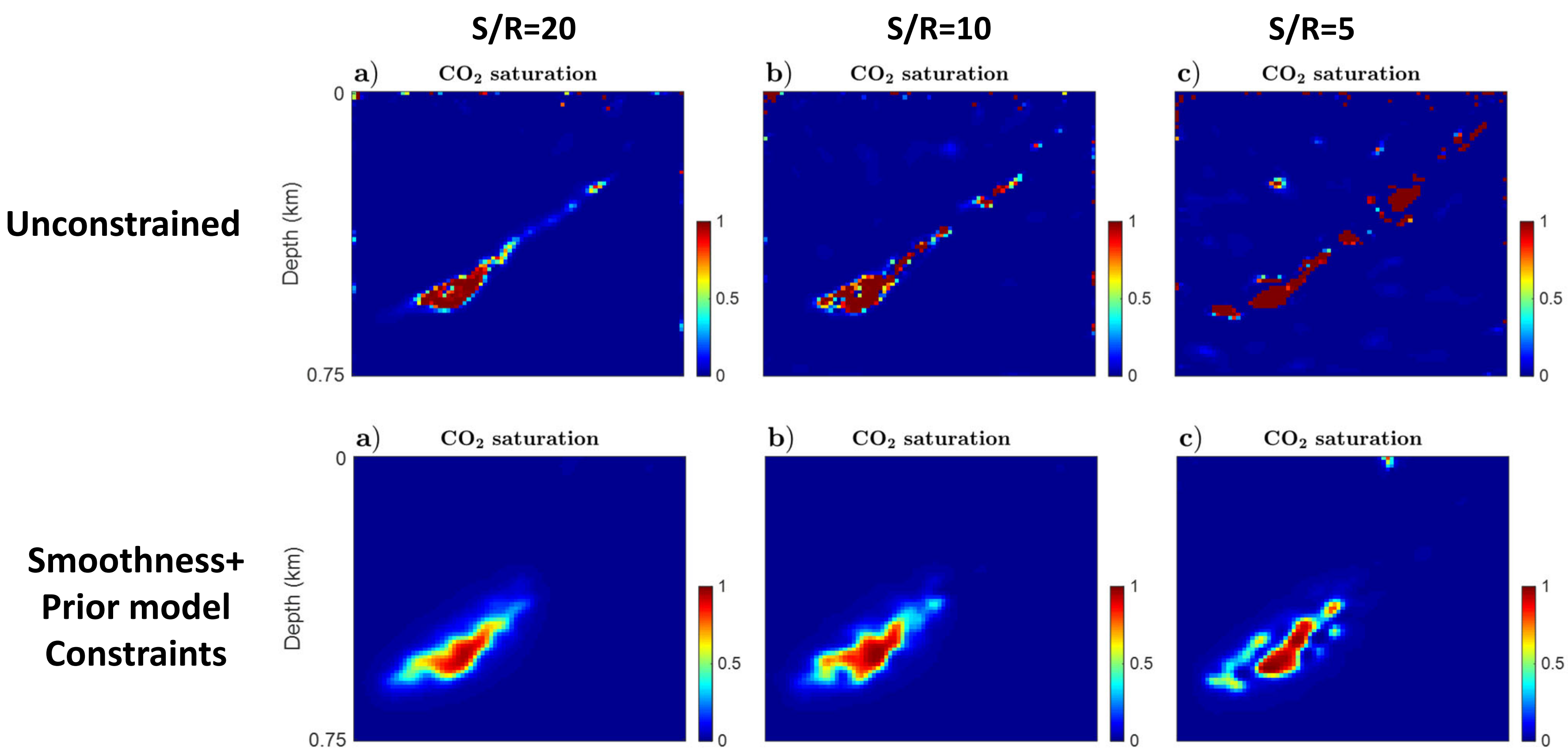

Summary in this part

True

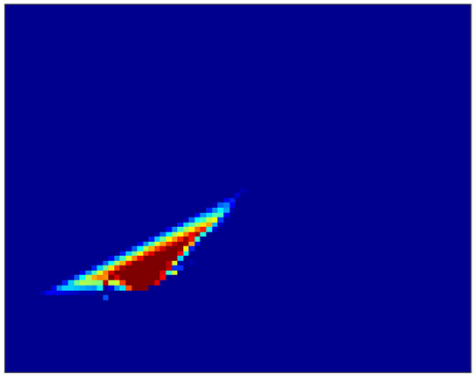

Errors in baseline models

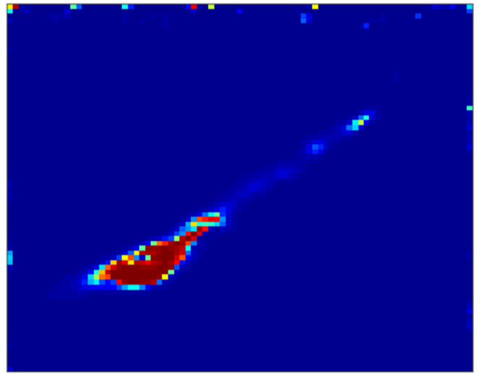

Errors in baseline models + random noise

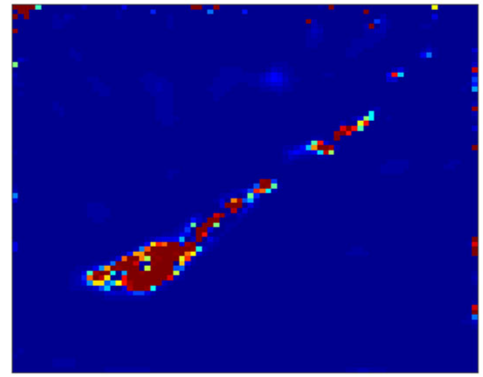

Smoothness constraint

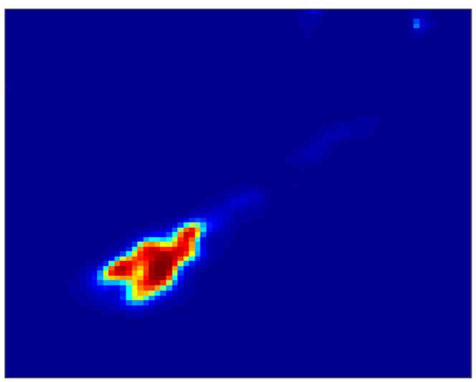

Prior model constraint

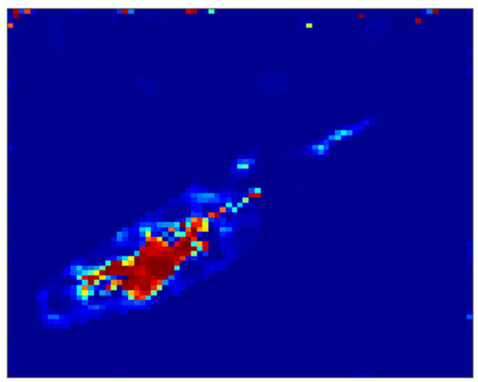

Smoothness + prior model constraints

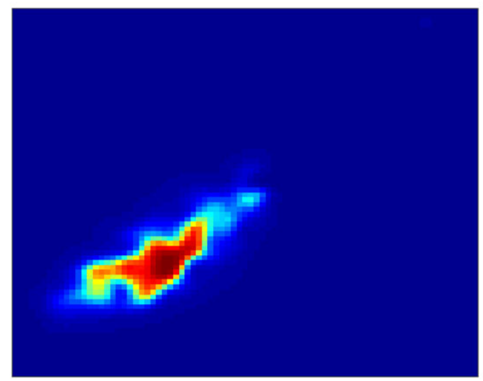

Summary of inversion results

True

Recovered

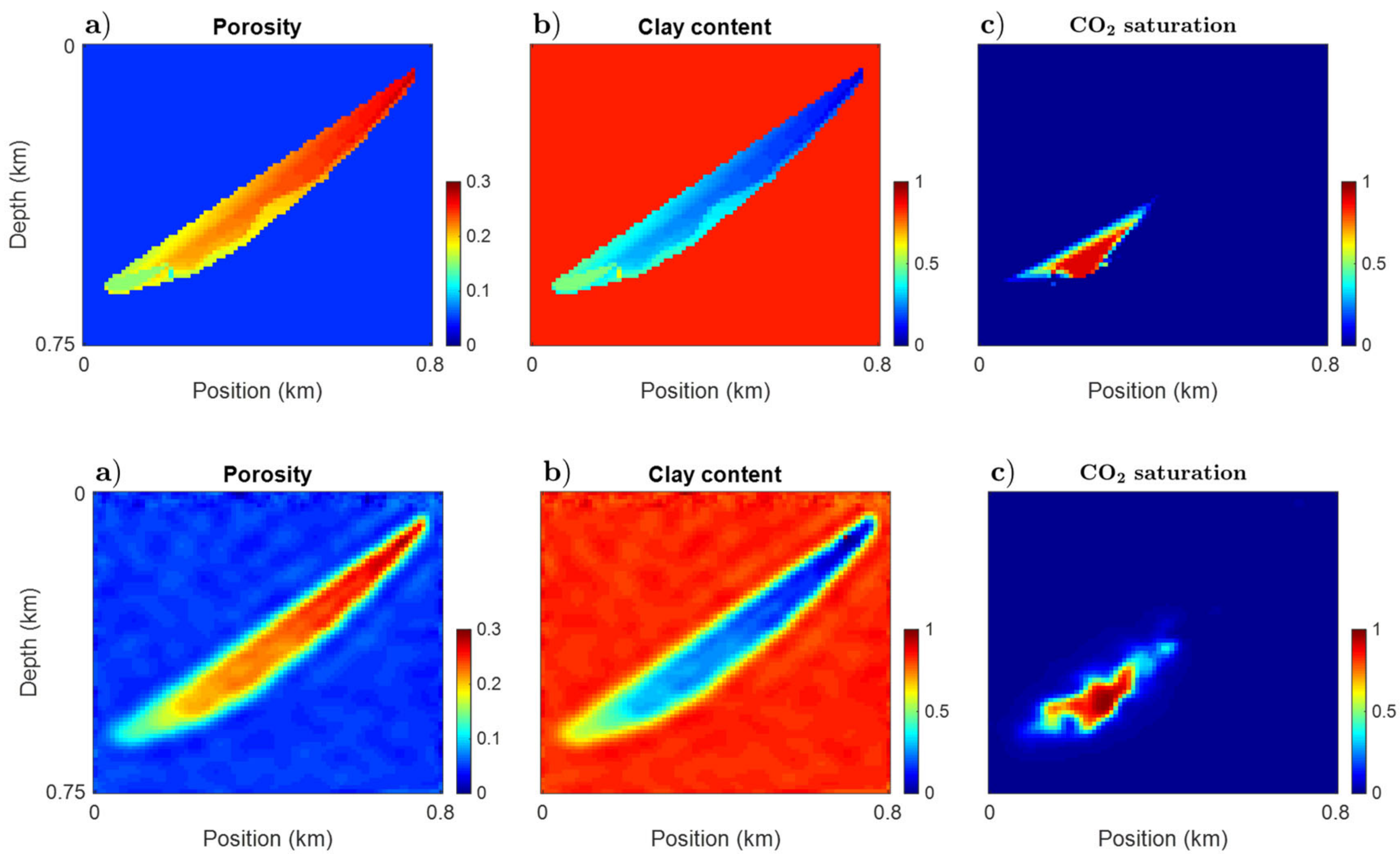

Summary

- We present an FWI method for the prediction of porosity, lithology and time-dependent CO_2 saturation values from seismic data.
- We show that the errors in baseline model estimates and random noise effects both compromise the estimation of CO_2 .
- We show that imposing model constraints, such as smoothness and prior model, can improve the result.

Acknowledgments

- Dario Grana
- CREWES sponsors, staff, and students.
- NSERC (Grant CRDPJ 543578-19)